

STABILITY SCREENING OF ARRAYS OF MAJOR HISTOCOMPATIBILITY COMPLEXES ON COMBINATORIALLY ENCODED FLOW CYTOMETRY BEADS.

Shi Ling Chew^{1,4}, Ming Yan Or^{1,4}, Cynthia Xin Lei Chang^{1,2}, Adam J. Gehring³, Antonio Bertoletti³, Gijbert M. Grotenbreg^{1,2,*}

From the *National University of Singapore (NUS)*¹, *Department of Microbiology, Department of Biological Sciences, and Immunology Programme, Life Sciences Institute, #03-05, 28 Medical Drive, 117456 Singapore*, the *NUS Graduate School for Integrative Science and Engineering (NGS)*², *Life Sciences Institute, #05-01, 28 Medical Drive, 117456, Singapore*, and the *Singapore Institute for Clinical Sciences (SICS)*³, *Agency for Science Technology and Research, Brenner Centre for Molecular Medicine, 30 Medical Drive, 117609, Singapore*. Both authors contributed equally to this work⁴

Running Title: Stability Screening of MHC Arrays on Encoded Beads

Address correspondence to: Gijbert Grotenbreg, Immunology Programme, Centre for Life Sciences #03-05, 28 Medical Drive, Singapore 117456, DID: (+65) 6516 6661, Fax: (+65) 6778 2684, Email: grotenbreg@nus.edu.sg

SUPPLEMENTAL FIGURE LEGENDS

SUPPLEMENTAL FIGURE S1. Fluorescence of beads in multiple flow cytometry channels. The odd numbered peaks of fluorescent particles sets Yellow, Pink, and Blue were measured in all channels on an LSR-II (Becton Dickinson) flow cytometer. The exact laser and filter set-up of the flow cytometer used for analysis is indicated by (a) the excitation lasers (b) the band pass filters (c) the common chromophore detected in that channel. Histograms with a black background indicate no appreciable fluorescence above background in that particular channel, whereas histograms with a white background indicates detectable fluorescence in that particular channel.

SUPPLEMENTAL FIGURE S2. Fluorescent bead assay compared to ELISA. Results obtained for stabilization of (a) human HLA-A*02:01, (b) murine H-2K^b, and (c) murine H-2D^b by fluorescent bead assay (left column) were compared by running the identical experiment using the conventional enzyme linked immunosorbent assay (ELISA) format (right column) as described by Rodenko *et al.* (1) The black bar graph (*) indicates that the H-2D^b control reaction was incubated at 50°C to drive complex disintegration to completion. No qualitative differences could be discerned.

SUPPLEMENTAL FIGURE S3. Fluorescent bead assay compared to ELISA. Results for (a) the alanine-scan, (b) the arginine-scan, and (c) the aspartic acid-scan of HLA-A*02:01 molecules that were ligand-exchanged with peptide derivatives of the known parent peptide ligand P10 obtained by fluorescent bead assay (left column) were compared by running the identical experiment using the conventional enzyme linked immunosorbent assay (ELISA) format (right column) as described by Rodenko *et al.* (1) No qualitative differences could be discerned.

SUPPLEMENTAL FIGURE S4A. Two dimensional coding of Yellow beads. The gating strategy is shown of the mixture of two-dimensionally coded beads, and the schematic of the combinatorial coding in two dimensions with an internal primary color and the secondary color on the bead's streptavidin-coated surface. Of the 12 individual populations of the Yellow beads a maximum of 11 peaks could be separated. As a result peak #2 was omitted because it too closely overlapped with peak #3. These 11 populations were coated in 3 different intensities with near-infrared (NIR) fluorescent reactive dye as the secondary color. The clear separation of the 33 individually coded populations could be accomplished in a single experiment. In this figure, the color schemes of the beads intensity are based not on physical appearance of the beads but on the emission properties. Dotted lines were drawn in arbitrarily after analysis to serve as visual aid and do not represent specific gates.

SUPPLEMENTAL FIGURE S4B. **Two dimensional coding of Pink beads.** The gating strategy is shown of the mixture of two-dimensionally coded beads, and the schematic of the combinatorial coding in two dimensions with an internal primary color and the secondary color on the bead's streptavidin-coated surface. The 12 individual populations of the Pink streptavidin-coated fluorescent particles were coated in 3 different intensities with near-infrared (NIR) fluorescent reactive dye as secondary color. This allowed the clear separation of a grand total of 36 individually coded populations in a single experiment. In this figure, the choice of color schemes of the beads intensity is based not on physical appearance of the beads but on the emission properties. Dotted lines were drawn in arbitrarily after analysis to serve as visual aid and do not represent specific gates.

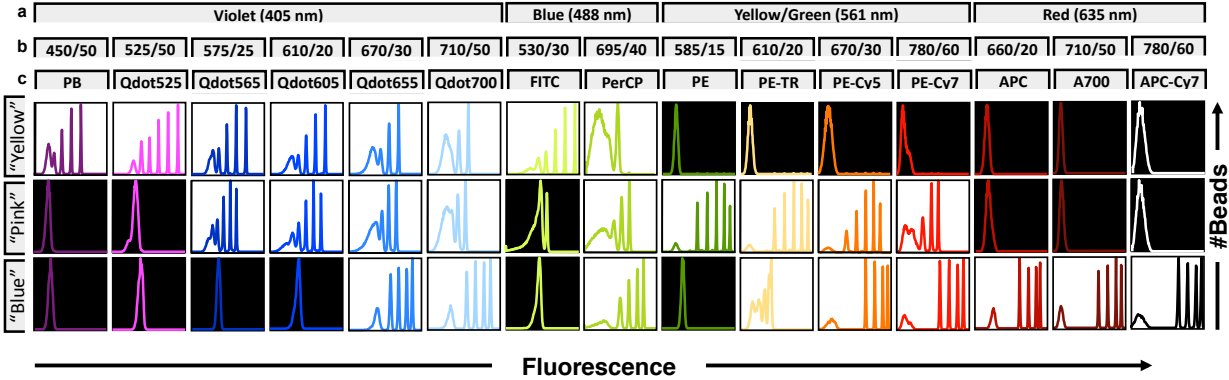
SUPPLEMENTAL FIGURE S4C. **Two dimensional coding of Blue beads.** The gating strategy is shown of the mixture of two-dimensionally coded beads, and the schematic of the combinatorial coding in two dimensions with an internal primary color and the secondary color on the bead's streptavidin-coated surface. The 10 individual populations of the Blue streptavidin-coated beads were coated in 3 different intensities with green fluorescent reactive dye as the secondary color. The clear separation of 30 individually coded populations in a single experiment was feasible. The choice of color schemes of the beads intensity, in this figure, is based not on physical appearance of the beads but on the emission properties. Dotted lines were drawn in arbitrarily after analysis to serve as visual aid and do not represent specific gates.

SUPPLEMENTAL FIGURE S5. **Stability of secondary color.** The individually coded populations as described in Supplemental Figure 4 for (a) Yellow, (b) Pink, and (c) Blue beads were stored at 4°C and shielded from light for several weeks and the individual fluorescence was measured at the indicated timings. From this experiment no appreciable decay of fluorescence can be observed for the Low, Medium, or High populations of secondary color.

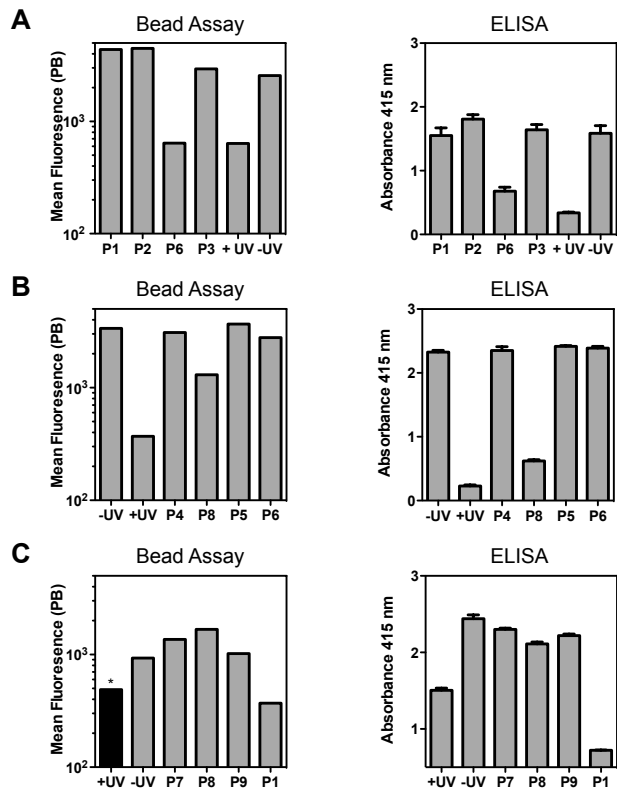
REFERENCES

1. Rodenko, B., Toebes, M., Hadrup, S. R., van Esch, W. J. E., Molenaar, A. M., Schumacher, T. N. M., and Ovaa, H. (2006) *Nat Protoc* **1**, 1120-1132

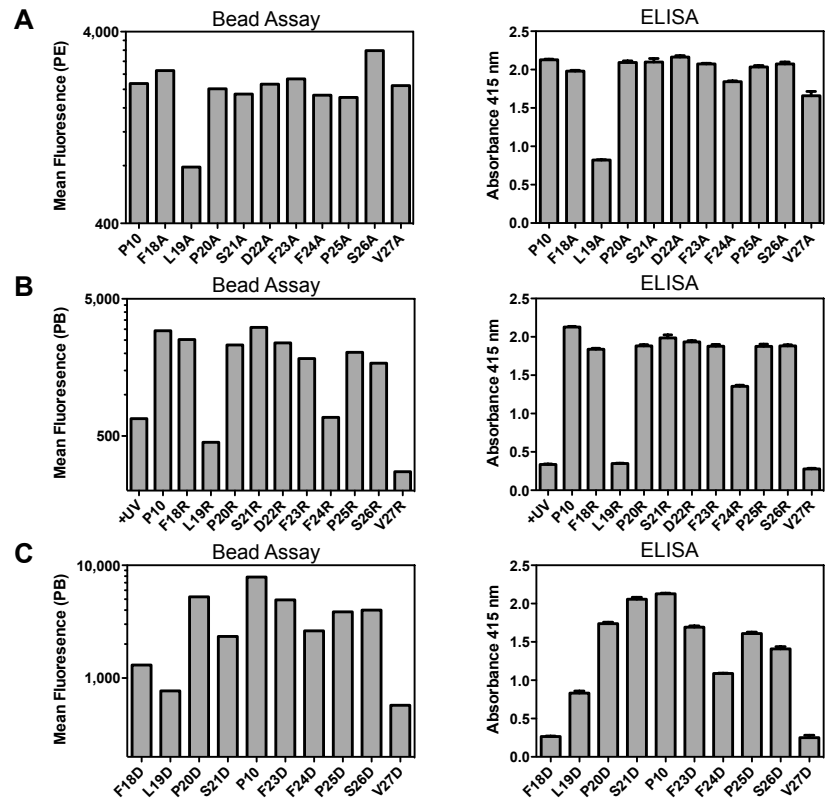
Supplemental Figure S1:



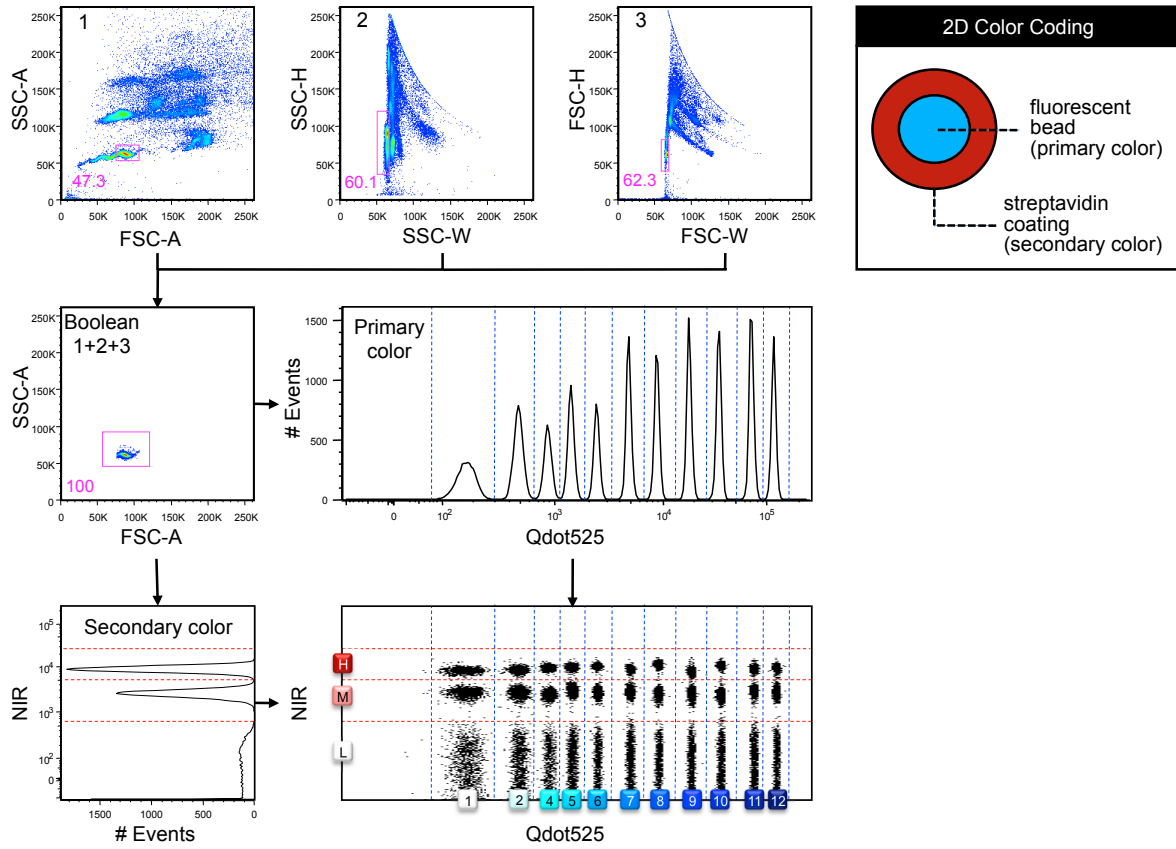
Supplemental Figure S2:



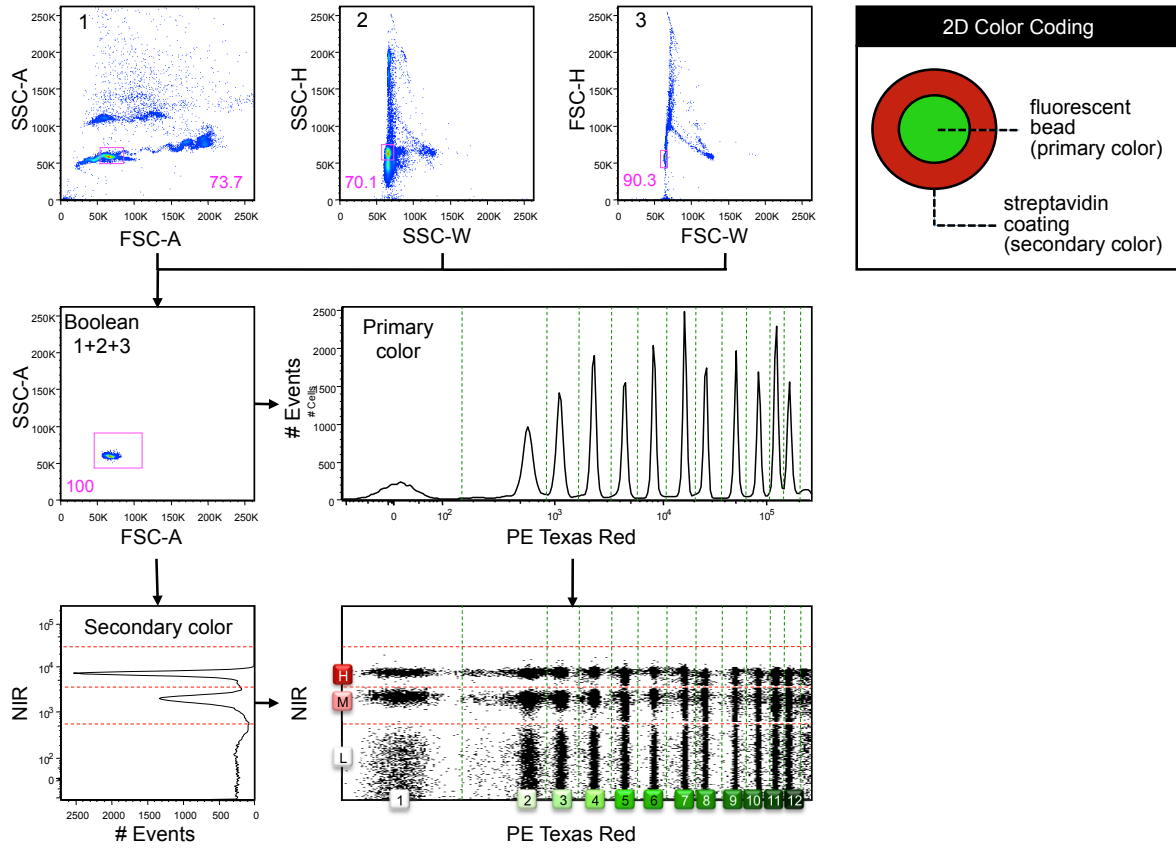
Supplemental Figure S3:



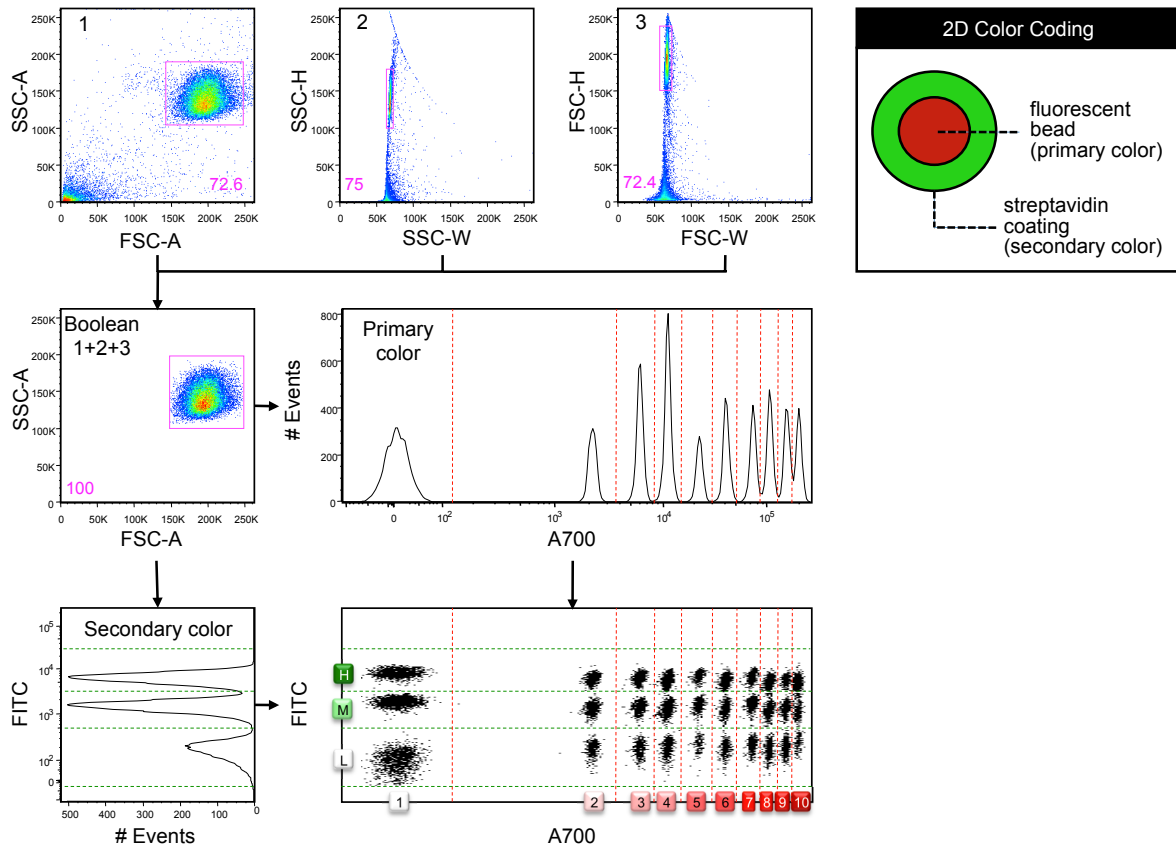
Supplemental Figure S4A:



Supplemental Figure S4B:



Supplemental Figure S4C:



Supplemental Figure S5:

